Article

Microscopic Kinetic Data on Crystal Growth from Macroscopic Morphology

Gergely To#th

Cryst. Growth Des., **2008**, 8 (11), 3959-3964 • DOI: 10.1021/cg800005g • Publication Date (Web): 10 September 2008

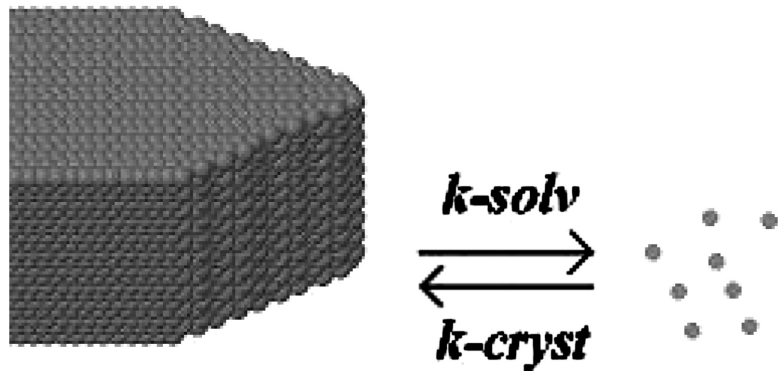

CRYSTAL GROWTH & DESIGN
2008
VOL. 8, NO. 11
3959–3964

Microscopic Kinetic Data on Crystal Growth from Macroscopic Morphology

Gergely Tóth*

Institute of Chemistry, Loránd Eötvös University, H-1518 Budapest, P.O. Box 32, Hungary

Received January 3, 2008; Revised Manuscript Received June 25, 2008

ABSTRACT: The macroscopic shape of crystals is determined by atomic and molecular processes. This concept is used in most of the theoretical and computational studies on crystal growth, where macroscopic morphology is predicted on the basis on microscopic properties. We were interested in the opposite direction, how one could get information on the microscopic processes with the knowledge of the macroscopic crystal shape. We combined the genetic algorithm and kinetic Monte Carlo simulations to determine molecular rate constants on the crystal growth of urea in water and in methanol. The input data were the macroscopic morphology and the structure of the unit cell. Surprisingly, our reaction rates corresponded well to data obtained in a recent study starting from molecular interactions. Our result showed numerically, that the morphology of a crystal contains relevant and recoverable information on microscopic crystal-growth processes.

Introduction

The macroscopic shape of a crystal depends on many factors, for example, on the concentration of the solute, on the temperature, on the properties of the solvent and on the presence of impurities and substrates, where heterogeneous crystallization may occur. These factors vary the rates of the possible local surface reactions and open different reaction routes. The entirety of the kinetic processes materializes in the macroscopic morphology. Most of the theoretical and computational studies concerning nucleation and crystal growth start at interactions, for example, see refs 1−5. Traditionally, macroscopic properties are taken into account, but recently, more emphasis is put on the interactions at the atomic/molecular level. On the contrary to it, we present a study, where starting from the macroscopic morphology and the structure of the unit cell we derived rate constants for microscopic processes. Our rates are similar to those ones obtained in the investigations of Piana and Gale[6−8] starting from molecular interactions.

We mention some aspects of crystal-growth modeling with microscopic interactions before the description of our method. In the case of computational modeling on crystallization, a key concept is the determination of the relevant microscopic processes together with their kinetic rates.[3]

A possible way is the use of dynamic simulations to recognize the processes. The system evolves in the crystal growth or dissolution direction in the simulations, and track if kept of the moves of the particles.[3,6−8] The elementary reactions can be identified by applying numerical criteria for the displacements or by visualizing the moves by sequences of snapshots. Unfortunately, the time domain of the dynamic simulations is restricted. Only a few events can be observed during a simulation, and the original method cannot be applied for rare processes. The size of the simulated systems is restricted as well. It usually contains only a part of the crystal, for example, a surface with few kinks and edges. It limits the number of the possible processes because some reaction routes can be identified only in simulations where different surfaces or large-scale crystal defects, for example, screw locations, are present. Reasonable time domain and simulation cell size can be achieved for some systems, if classical mechanical interactions (empirical potentials) are used together with further approximations, for example, on the solvent. Unfortunately, simple models cannot reflect all properties of the substances, which can be essential for the development of many reaction routes. In the case of sophisticated interaction models, the time and size limits of the simulations decrease drastically. If quantum mechanical calculations (first principles methods) are used on the fly, the system size is restricted up to a few hundred atoms and the upper time limit is a few nanoseconds.

Another way is the determination of a part of the potential-energy landscape and vibration properties in calculations concerning few points of the phase space, for example, see ref 3. The rate constants can be calculated using the transition state theory,[9] if the potential energy and the harmonic vibrations of the initial point and the saddle point are known.[10] The search for the transition pathways needs sophisticated algorithms and a reliable initial guess about them.[3] Unfortunately, if first principles calculations are used, the system can be even smaller than to be able to adequately represent a crystal surface. Another choice is to map the free-energy landscape of the crystal surfaces together with the contacting solvent. In the case of first principles methods it seems to be intractable nowadays. In the case of empirical interactions and classical dynamics, there is a possibility to use accelerated dynamics[11] or metadynamics.[12] It is an advantage of the potential energy and free energy maps that they do not depend on the real time scale of the crystalline processes. Therefore, the determination of the maps is possible for slowly crystallizing materials as well.

If all relevant microscopic events and rates are known, the mesoscopic (10^{-8}−10^{-5} m) structure of a crystal can be modeled in kinetic Monte Carlo (KMC) simulations.[3,13−16] Here, elementary processes are performed at randomly selected crystal positions of a super cell. A process occurs proportional to its rate constant. Usually, trivial processes are chosen, like intake of a solute entity to the crystal surface, dissolution of a crystalline particle, or surface diffusion of a particle. The rate constants are unlike for sites with differently occupied neighbor positions. The super cell may consist of a few hundred to million unit cells of the crystal. A small part of the lattice points are filled with molecules at the start, and this seed grows during the KMC simulation. If the middle of the super cell is filled at the start, three-dimensional crystal growth can be simulated.

* To whom correspondence should be addressed. E-mail: toth@chem.elte.hu.

10.1021/cg800005g CCC: $40.75
Published on Web 09/10/2008

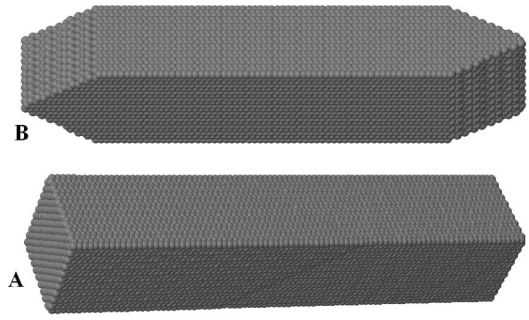

Figure 1. Schematic view of urea crystals in water (A) and in methanol (B).

The crystal growth on a special surface can be simulated, if there is surface, which goes through the super cell and it is filled fully with particles at the start. In this case, the super cell can be abandoned with its periodic replicas, as well. The reality of the KMC modeling depends on the choice of the elementary processes and the authenticity of rate constants.

Piana and Gale[6−8] combined classical molecular dynamics and KMC simulations to study the crystal growth of urea in two solvents. Urea forms rectangular crystals in water; needle like tetragonal ones can be obtained with large *c*/*a* cell-axis direction ratio.[4,7,17,18] In methanol the [001] faces are displaced by the [111] faces in V-formation and the two wedges are rotated with 90 degrees with respect to each other at the opposite ends of the crystal.[7,17,18] In Figure 1 the two crystals are schematically sketched with a smaller *c*/*a* direction ratio than it is experimentally observed. Piana and Gale performed molecular dynamics simulations with empirical potentials on systems containing a given surface of urea crystals and solvated urea. They determined the rate constants of the many possible elementary reactions by counting the events during the dynamical simulations. Thereafter, they performed KMC simulations with these rate constants. In the KMC simulations they were able to reproduce the shape variety of urea caused by the solvents.

Piana and Gale showed that the macroscopic crystal structure can be understood and reproduced on the basis of microscopic interactions, and the reaction rate constants obtained for microscopic processes are reliable. We started from a different hypothesis in our study, namely, that simply the macroscopic morphology of a crystal might help to recognize the main kinetic features of the microscopic processes. To say it in another way: microscopic kinetics determines the macroscopic morphology. How does it work in the reverse direction?

Details of the Calculations

Urea crystallizes in the space group $P\bar{4}2_1m$. The unit cell contains two molecules.[19,20] We categorized the lattice points according to the occupation of the neighboring positions. A urea molecule is connected to six molecules with hydrogen bonds (Figure 2). If *x*, *y*, and *z* directions are parallel to the *a*, *b*, and *c* unit cell axis, the central urea molecule is a H-donor in the $-z$ direction ("A"-type neighbor) and an O-donor to the hydrogen bond in the $+z$ direction ("B"). There are four hydrogen bonds in the $x-y$ plane, the central molecule is a H-donor in two of them ("1") and an O-donor for the other two ("2"). Piana and Gale denoted the surrounding occupation by the presence of these codes, and we applied the same method. For example, 1122AB marks a lattice point where all neighboring positions are occupied. There are 36 different environments, if the similar positions (1−1 or 2−2) are not distinguished. If one takes into account a dissolution event and a crystallization one for each site, and processes for the sites with zero occupied neighbors or with fully occupied surrounding are not permitted, the number of the rate constants is 68 in a given solvent.

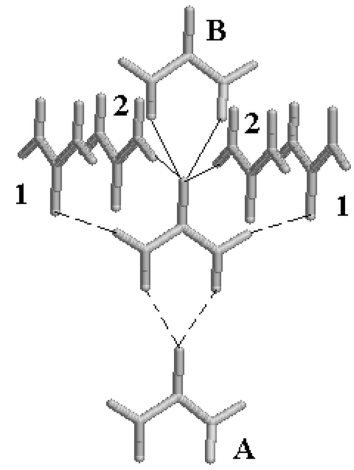

Figure 2. Six hydrogen-bonded neighbors of a urea molecule. The hydrogen bonds are denoted by solid lines, if the central molecule is an O-donor and by dashed lines if the central molecule is a H-donor.

Piana and Gale used a further distinction of the sites on the basis on a pseudo second neighbor occupation. They defined 56 different environments resulting in 108 rate constants. Their definition splits 10 of our positions to 30 ones. In any comparison of their and our rates, one can count a part of our rate constants as the average of of three constants defined by Piana and Gale.

We optimized the rate constants on the basis on macroscopic morphology. A combination of genetic algorithm, as a parameter optimizing method, and KMC simulations was applied. The population consisted of 20 rate constant sets in the genetic algorithm. The 20 initial sets of kinetic parameters were created randomly. One set contained 68 parameters due to the nearest-neighbor definition detailed above. A fitness function (*F*) was calculated for each set as the overlap integral of the idealized target crystal and the crystal grown in a kinetic Monte Carlo simulation with the given rates. The target crystals are detailed later. The overlap was counted as the number of the occupied lattice points in the crystals grown in the KMC simulation, which points were within the target crystals. The overlap integral was normalized with the number of the occupied lattice points in the idealized crystal. Therefore, the fitness value was in the [0;1] range, where 1 meant the perfect reproduction of the idealized target. The modification of the rate constant sets was performed in survival, replication, crossover, and mutation steps. The two best sets survived and appeared in the next population. Further two sets were replicated into the next population by choosing them randomly proportional to their *F*-*F* (worst in the population) value. The remaining 16 sets were generated by crossover, where the rate constants for the same lattice site were randomly chosen from one of the parent's one, and the parents were randomly chosen proportional to their *F*-*F* (worst in the population) value. There was a mutation step, where all rates in the new population were mutated with a 0.1 probability by multiplication of a random number within the 0.2−1.8 range. Each parameter estimation with the genetic algorithm contained 500 subsequent populations. 15−20 optimizations were performed for each target crystal, whereof the best 10 calculations (= largest average *F*) were selected. The data shown in the figures were calculated as the average of the 20 rate sets of each of the selected 10 optimizations. It meant all together 200 sets for a target crystal. The fitness of the corresponding KMC grown crystals was larger than 0.9 for all of the 200−200 selected crystals in water and methanol solvents.

The kinetic Monte Carlo simulations were performed for each set of the rate constants. It means, that $20 \times 500 = 10000$ KMC calculations were performed in each parameter estimation. The total number of the KMC simulations was around 500 000 for the parameter estimations on different target crystals. Therefore, we were not able to choose a large super cell in the calculations. It contained $30 \times 30 \times 100$ unit cells of urea crystal. Each simulation started with a cubic nucleus filling 0.5% of the super cell. Both occupied and unoccupied lattice points were visited one after the other and an event might occur there proportionally to the rate constants. In the case of the crystal-

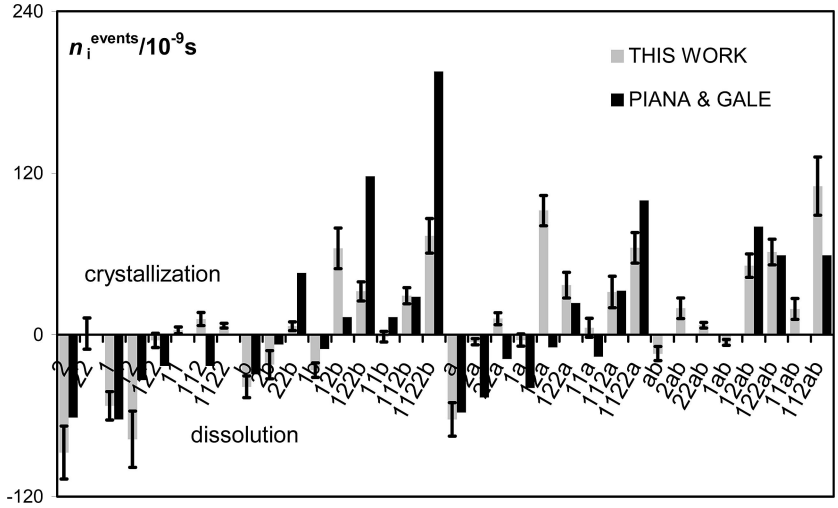

Figure 3. Expected number of events at different urea sites in water.

lization, the solute concentration appeared as a multiplicative factor in the probability. We did not predefine this concentration according to some experimental facts or theoretical assumptions (see, for example, Piana and Gale). We simply used it as a practical parameter to keep the ratio of the number of the crystallization events and the dissolution ones to be 1.05 during the KMC calculations. A KMC simulation was stopped if the size of the crystal reached the size (= number of occupied lattice points) of the target crystal or it reached the border of the super cell. Thereafter, the fitness value was calculated for this crystal. The shape of the crystals grown was spherical in the initial populations of rate constants. The elongation of the crystals in the z direction was visible after few genetic algorithm steps. The rectangular shape in the $x-y$ plane evolved around the 50−100th parameter changes of the genetic algorithm.

The target crystals mimicked the experimental shapes of urea in water and in methanol. They are shown in Figure 1. In the case of water solvent, the crystal was 41.8 nm × 7.5 nm × 7.5 nm and it was confined by (001), (110), and (1,−1,0) faces. It contained 36 000 urea molecules. In the case of methanol solvent, the two wedges were cut from the idealized crystal in water. Here, the (111), (11−1), (1−11), and (−111) faces bordered the crystal instead of the (001) ones. The target crystal for methanol solvent contained 30 320 urea molecules. Both crystals were placed in the center of the super cell with size of 30 × 30 × 100 unit cells. The experimental z/x ratio can be higher than 1000 for urea crystals in water. We were not able to define a target crystal with this axis ratio because the demand on computer memory and calculation time would increase intractably. We defined a rather small 6:1 ratio for our targets because this provided feasible calculation times. Of course, we checked the effect of this distortion. Some separate KMC simulations were performed with the best sets of rate constants in a super cell of 50 × 50 × 400 unit cells. We found that the sets optimized to targets with a ratio of 6:1 in a 30 × 30 × 100 unit cells size provided significantly larger (around 17:1) axis ratio in the large super cell. The similar effect was observed if we grew crystals with the rate constants of Piana and Gale. We achieved around 6:1 axis ratios in the 30 × 30 × 100 cell, but we got significantly larger (17−18:1) ratios in the large cell. We concluded that the choice of a target crystal with the small ratio in this small super cell was not a deceptive starting point because the crystals grown were closer to the real ratio in the large super cells. Maybe, there is a given size in the x and y direction that evolves fast in small crystals and thereafter the growth in the z direction becomes dominant. This type of kinetics seemed to be inherent in both our rates and the ones of Piana and Gale.

If a rate constant set is obtained with our process to reconstruct a macroscopic crystal shape, one has to scale it to the real growth rate because there is no explicit time in our parameter optimization. It means our method yields only relative rates rather than the rates themselves. The unit of the KMC simulation is one iteration, when all sites are sequentially visited and the possible processes are performed with a probability proportional to the rate constants. This time unit is denoted here as "it". For the sake of simplicity, we normalized the k_i-s. $\sum ki^{solv}$ = 1(it^{-1}) and $\sum ki^{cryst} = [S_0]$ (Å^6 it^{-1}), if $[S_0]$ was smaller than 1 Å^{-3}. The dimension of $[S_0]$ was particle/volume (Å^{-3}). In the opposite case, $\sum ki^{solv} = 1/[S_0]$ (Å^{-3} it^{-1}) and $\sum ki^{cryst} = 1$ (Å^3 it^{-1}). In this way, a reaction proceeded in our KMC method if a uniform random number from the [0;1) range was smaller than the corresponding rate constant. In the case of long crystals in one direction, one may define a growth rate v^{sim} in Å/it units. If one experimentally determines the same rate for a macroscopic (or mesoscopic) crystal for urea, see refs 17, 18, one can define a growth rate r^{exp} in Å/s units. The real-time rate constants can be obtained by multiplying the k_i-s with r^{exp}/v^{sim}. In the case of Figures 3, 4, 6, and 7, we did not apply the aforementioned scheme because there is a comparison of data sets from different origins in these figures. The number of the possible processes was smaller in the study of Piana and Gale than in our one because many of the possible rates were set to zero in their study. This difference in the models caused some arbitrariness in the comparison. Furthermore, we were not sure, whether we should have to use a r^{exp} determined by KMC simulations with the rates of Piana and Gale or we should have to find experimental data. The scaling of the rates shown is detailed with the discussion concerning the figures.

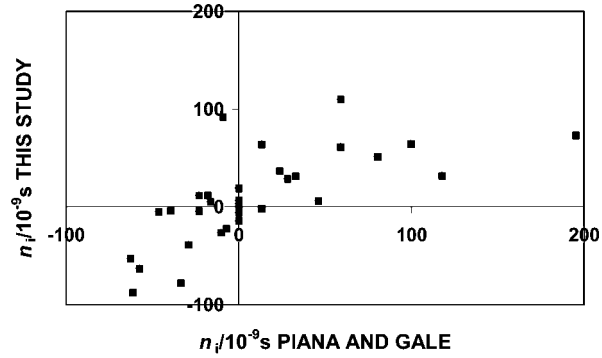

Figure 4. Scatter plot of the number of events at different positions between Piana and Gale and our study for urea crystals in water.

Results And Discussion

It is not easy to estimate how vague our combination of genetic algorithm and kinetic Monte Carlo simulation is for determining rate constants. It is a complex task to relate the information content of the input data (the morphology of a target crystal and the data of the unit cell) on the rate constant. We note here, that as a specialized case for crystallization, the task is philosophically similar to the Hohenberg−Kohn theorem[21] in quantum mechanics or Henderson's inverse theorem[22] of

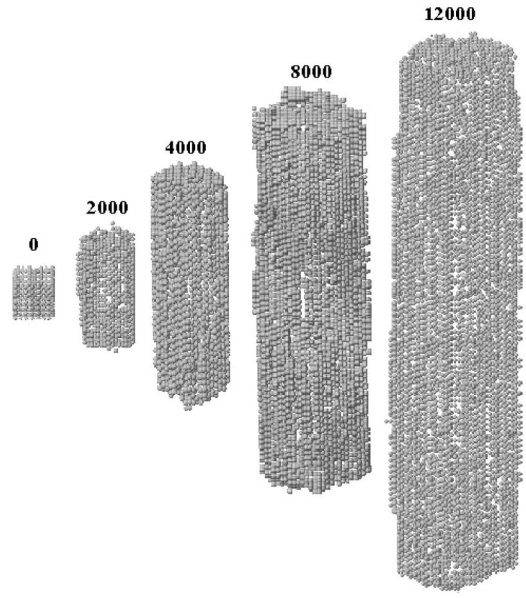

Figure 5. Crystal growth in a KMC simulation. The numbers denote the iterations in the KMC method. The rate constants were obtained for urea crystal in water with our method. The spheres represent the urea molecules.

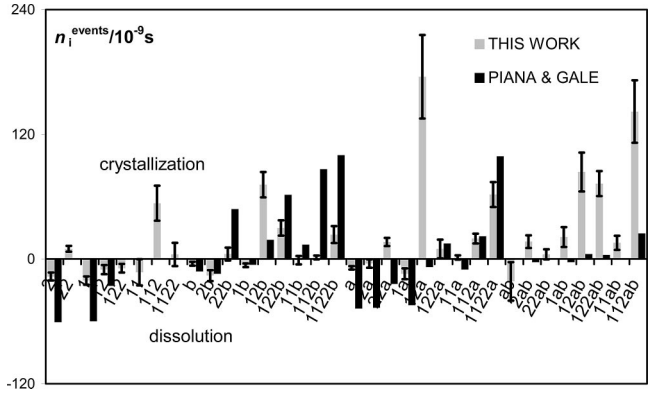

Figure 6. Expected number of events at different urea sites in methanol.

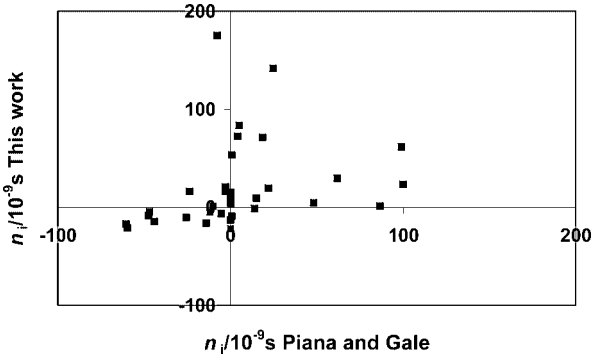

Figure 7. Scatter plot of the number of events at different positions between Piana and Gale and our study for urea crystals in methanol.

classical statistical mechanics. The number of the rate constants was 68, and we hardly expected to determine any unique or exact rate constant set. We thought that a large number of different combinations of the rates might result in the desired shape in the KMC simulations. The KMC method passes all of the surface positions in an iterative step. The possible crystallization or solution process is performed there according to the occupation state of a lattice point. If there is a change in the occupation state of a position in an iterative step, there is a possible backward reaction in the next step. The difference between the probabilities of the two reactions is characteristic for a given neighborhood. We calculated this expected number of events as $n_i = k_i^{cryst} \times [S_0] - k_i^{solv}$ for the different sites. It shows that the crystal tends to grow or dissolve at the *i*-th type of lattice position. The expected number of events (positive means crystallization, negative means dissolution) is a net kinetic rate constant and it can be considered as a driving force in the KMC simulation. It is not a thermodynamic property, but it is a kinetic property. Its use does not conflict with the general scheme that crystal growth is a kinetically controlled process. The same value can be obtained by rates with different magnitudes because the expected number of events is a difference between the forward and backward rates. Therefore, the determination of the exact elementary rate constants is close to impossible in any parametrization method using KMC simulation. There was a hope only to determine these net rate constants in our method. It means a reduction of the task to explain and to discuss only these 34 independent features in our case.

The average n_i-s are shown for water together with the confidence intervals of 0.05 significance in Figure 3. The data were calculated over the selected 200 rate sets detailed in the previous section. Despite the differences of the models, the n_i values of Piana and Gale are shown for comparison as well. If three rate constants were published for a given first-neighbor environment by Piana and Gale, according to their second-neighbor environment, their average was used for the figures. In Figure 3 (and also Figures 4, 6, and 7) we scaled our data to provide the same value for $\sum|ni^{events}|$ as it can be calculated for the rate constants of Piana and Gale.

The most important feature is the direction of the net effect at a given site. Positive means crystallization and negative means dissolution. The trends are expressively similar in the two sets of net rates. We show the rates from the two sources with respect to each other in Figure 4. The rates of Piana and Gale are used as *x* values and our ones as *y* values. The two sets reflect the same directions for most cases, and their extents are close to each other. There are disagreements in the data as well. There are eight cases where Piana and Gale did not observe an event during the molecular dynamics, and the corresponding rates were set to zero. We did not assume any restriction on the positions except that a fully coordinated site could not change its occupancy. Of course, our nonzero rates at the positions assigned to zero by Piana and Gale could be simple artifacts of the parameter optimization. They can be interpreted in another way as well, namely, that these rates belong to composite processes. An example can be a change at a shielded position, where at first the shield removes, then the change occurs, and finally the shield recovers. There is another type of difference in the two sets: an opposite direction of the expectable process. One can find five such net rates. A part of these lattice points is within the statistical error bars of the parameter fit, but in some cases, the differences are significant. It might be caused by the lack of the spatial physics and interactions in our modeling. We might summarize that from the 34 n_i values 21 showed the same direction, 8 data could not be compared according to the different model (zero in Piana and Gale's study), and 5 points were guessed in the opposite direction. The correlation coefficient was 0.69 for the two sets if we used all data points. If we omitted the 8 zero values and the 5 badly estimated data,

the correlation coefficient was 0.78. If we took into account only the sign of the net rates and we omit the net rates defined zero by Piana and Gale, we were able represent the two data sets as binary ones. The Tanimoto distance (for example, see ref 23) of the two binary sets was 0.19. It means that 81% of the net rates showed the same direction in the two sets. The corresponding Hamann association coefficient (for example, see ref 23) was 0.61. The Hamann association coefficient reflects similar features for binary variables as the correlation coefficient for continuous variables.

A snapshot sequence of a KMC simulation is shown in Figure 5. The rate constant set applied is one of the 200 "best sets" chosen in the statistical analysis. The shape of the initial seed was cubic with (100), (010), and (001) faces. The cube grew significantly in the z direction and "turned" around the z axis (more precisely evolved in the $x-y$ plane) to mimic the urea crystals in water already after a few thousands of KMC iterations. The ratio of the growth in the z direction versus x or y directions is more emphasized with increasing crystal size.

The results for methanol are shown in Figures 6 and 7. The quantitative agreement was less pronounced for the two sets. For example, we obtained large net rates for sites where Piana and Gale did not observed reactions. Of course, most of our data for urea in methanol resembled those for urea in water because the two crystals are similar except for the form at the ends of the crystals. The differences between our and the molecular dynamics data in methanol were like to the ones observed in water, and they could be explained similarly. Here, six rates were set to zero by Piana and Gale. Our net rates were different in signs at six types of neighborhoods. If we summarized the data on urea in methanol, from the 34 n_i values 22 showed the same direction, 6 data could not be compared according to the different model (zero in the study of Piana and Gale), and 6 points were guessed in the different direction.

The correlation coefficient was 0.28 for all of the data, and it was 0.40 if we omitted the values set to zero by Piana and Gale and the net rates, which were guessed in the wrong direction. If we used only the signs of the nonzero coefficients as binary variables, the Tanimoto distance of the two sets was 0.21. It meant, that the 79% of the net rates showed the same direction in the two sets. The corresponding Hamann association coefficient was 0.57. The Hamann association coefficient of the binary variables was significantly larger than the correlation coefficients of the original net rates. It reflected that the quantitative agreement between the two sets was weaker than the qualitative one if we defined that the quantitative term belonged to the magnitudes of the net rates and the qualitative term belonged to the sign of the net rates. In the case of urea in water, the two sets provided similar correlation and Hamann coefficients. It could be interpreted as a similar level of qualitative and quantitative agreements between the two sets. For comparison we calculated these coefficients for the water−methanol data pairs for our and in Piana and Gale study as well. The net rates of our study are shown for the two solvents in Figure 8. The correlation coefficient was 0.86 and the Hamann coefficient was 0.85 between the two solvents in the study of Piana and Gale. They were 0.79 and 0.94 for the two solvent in our rates. It meant that both the interaction based study of Piana and Gale and our numerical parametrization investigation provided similar results for the two solvents.

The rate constants highlighted characteristic differences between water and methanol kinetics, which are responsible for the V-formations at the ends of the crystals. For example, there are four sites (112, 122, 1AB, and 2AB) where zero or quasi

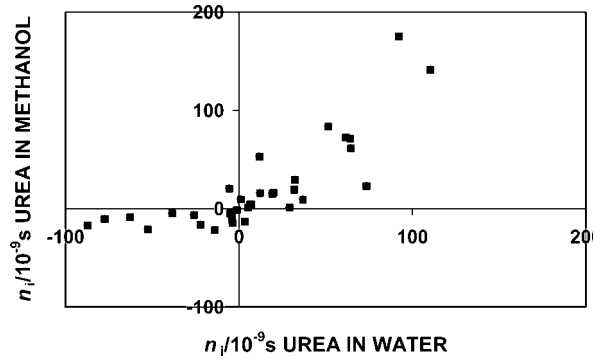

Figure 8. Scatter plot of the number of events at different positions between the data for the two solvents in our study.

zero net rates changed to significant ones in the study of Piana and Gale. In our case, there were two sites with different signs of net rates for the two solutions (Figure 8.). They were the 1AB and 11 cases, whereof the 1AB was recognized as well by the other study. We should note that all of these sites had less occupied neighborhoods.

Conclusion

In the case of crystal growth, it is widely accepted that the microscopic interactions and processes determine the macroscopic morphology. The development of theories and computational methods provide many possibilities to apply this concept in the modeling of crystallization. Microscopic kinetic processes with appropriate rate constants are used as inputs in many of the applications, and the results are mesoscopic or macroscopic images of the crystals. We were interested in the reverse of this concept in our study, namely, what the information content of the macroscopic morphology is concerning the microscopic kinetics. We developed a method with the combination of genetic algorithm based parameter estimation and kinetic Monte Carlo simulations, where the input data were the structure of the unit cell and the macroscopic morphology. The aim of the method was to determine rate constants of microscopic processes on the basis on macroscopic structure. Our study concerned the crystal growth of urea in water and in methanol, where two slightly different morphologies were expected with the same unit cell. This system was chosen because rate constants were derived for it in a recent study of Piana and Gale. They derived the rates on the basis on molecular interactions. Surprisingly, our method provided similar rate constants for the elementary processes. The net rate constants (the difference in the expected number of crystallization or dissolution events at a lattice position with a given occupation of neighbors) were at least qualitatively similar in the interaction based study and in our one. The estimated directions of the processes at the positions coincided mostly for the 34 different cases. In the case of urea crystals in water, there was quantitative accordance as well.

Our calculations clearly showed that the macroscopic morphology of a crystal contains relevant and recoverable information on the rate constants of microscopic processes. The combination of genetic algorithm and the KMC simulation seemed to be an efficient tool to get the parameters. The agreement between the data of Piana and Gale and ours validated both methods: their molecular level interaction based microscopic dynamic model and our one starting from macroscopic morphology.

Acknowledgment. We are grateful for the financial support of the Öveges Grant OMFB-01412/2006.

References

(1) Liu, X. Y.; Boek, E. S.; Briels, W. J.; Bennema, P. *Nature* **1995**, *374*, 342–345.
(2) Engkvist, O.; Price, S. L.; Stone, A. J. *Phys. Chem. Chem. Phys.* **2000**, *2*, 3017–3027.
(3) Jonsson, H. *Annu. Rev. Phys. Chem.* **2000**, *51*, 623–653.
(4) Bisker-Leib, B.; Doherty, M. F. *Cryst. Growth Des.* **2001**, *1*, 455–461.
(5) Boerrigter, S. X. M.; Josten, G. P. H.; van de Streek, J.; Hollander, F. F. A.; Los, J.; Cuppen, H. M.; Bennema, P.; Meekes, H. *J. Phys. Chem.* **2004**, *108*, 5894–5902.
(6) Piana, S.; Gale, J. D. *J. Am. Chem. Soc.* **2005**, *127*, 1975–1982.
(7) Piana, S.; Reyhani, M.; Gale, J. D. *Nature* **2005**, *438*, 70–73.
(8) Piana, S.; Gale, J. D. *J. Cryst. Growth* **2006**, *294*, 46–52.
(9) Keck, J. C. *Adv. Chem.* **1967**, *13*, 85.
(10) Voter, A. F.; Doll, D. *J. Chem. Phys.* **1985**, *82*, 80–92.
(11) Voter, A. F. *J. Chem. Phys.* **1997**, *106*, 4665–4677.
(12) Laio, A.; Parrinello, M. *Proc. Natl. Acad. Sci. U.S.A.* **2002**, *99*, 12562–12566.
(13) Gillespie, D. T. *J. Comp. Phys.* **1976**, *22*, 403–434.
(14) Gilmer, G. H. *Science* **1980**, *208*, 355–363.
(15) Voter, A. F. *Phys. Rev. B* **1986**, *34*, 6819–6829.
(16) Fichthorn, K. A.; Weinberg, W. H. *J. Chem. Phys.* **1991**, *95*, 1090–1096.
(17) Boomadevi, S.; Dhanasekaran, R.; Ramasamy, P. *Cryst. Res. Technol.* **2002**, *37*, 159–168.
(18) Mougin, P.; Wilkinson, D.; Roberts, K. J. *Cryst. Growth Des.* **2003**, *3*, 67–72.
(19) Swaminathan, S.; Craven, B. M.; McMullan, R. K. *Acta Crystallogr.* **1984**, *B40*, 300–306.
(20) Swaminathan, S.; Craven, B. M.; McMullan, R. K. *Acta Crystallogr.* **1984**, *B40*, 398–404.
(21) Hohenberg, P.; Kohn, W. *Phys. Rev. B* **1964**, *136*, 864.
(22) Henderson, R. L. *Phys. Lett. A* **1974**, *49*, 197–198.
(23) Frank, I. M.; Todeschini, M. Data Handling in Science and Technology. In *The Data Analysis Handbook*; Elsevier: Amsterdam, 1994; Vol. 14.

CG800005G